Sensor placement technique using $BaTiO_3$/epoxy resin piezoelectric composite sensors based on image differential method for damage detection in structural health monitoring

Adrià TALTAVULL CAZCARRA [1], Oscar BAREIRO FERREIRA [1], Ramanan SRIDARAN VENKAT [1], Jens ADAM [2], Christian BOLLER [1]

[1] Non-Destructive Testing and Quality Assurance (LZfPQ), University of Saarland, Campus Dudweiler, 66125 Saarbrücken, GERMANY c.boller@mx.uni-saarland.de
[2] Leibniz Institute for New Materials (INM), Optical Materials Group, Campus D2 2, 66123 Saarbrücken, GERMANY

Key words: structural health monitoring, simulation of guided waves, image differential method, sensor placement.

Abstract

Structural Health Monitoring (SHM) is an emerging technology in many engineering disciplines that aims at designing systems being able to continuously monitor the aging of structures throughout their life span. Damage monitoring using guided waves (GWs) is one promising approach in that regard. In this article a network of integrated piezoelectric transducer patches is attached to a structure to generate GWs, which in turn propagate through the structure and information relative to the damage is recorded. Based on damage mechanics principles and damage tolerance criteria *the structure's remaining useful life* is to be then determined from the data recorded by the transducers and the need for structural maintenance actions can finally be derived accordingly. The detectability of the growing structural damage is highly dependent on the placement of actuators and sensors. This therefore requires an optimum placement of those transducers which is obtained through simulation. The requirement of simulation becomes specifically relevant when structures are large and complex. In this paper, a new approach to the sensor placement is introduced. This technique is based on the image differential method. The differential is determined from the difference of the wave patterns between an undamaged and a damaged condition. The resulting topology of the differential image is considered to define the shape/pattern of the respective piezoelectric transducers. An FEM model has therefore been developed to obtain numerically simulated differential patterns, which are generated for a pristine and damaged condition of a metallic plate. These differential patterns are taken as a basis to configure a sensor pattern that allows reliable damage detection. The model is based on a thin aluminum test coupon with three holes where a crack of tolerable length has originated from one of the holes due to fatigue loading. The piezoelectric composite transducer pattern for monitoring the crack has been defined from the output of guided wave FEM simulations.

1 INTRODUCTION

Non-destructive evaluation (NDE) methods are a reliable, efficient and economical approach to increase safety and reduce maintenance costs of structures. NDE techniques not only make early damage detection without compromising the integrity of the inspected structure possible, but also offer great accuracy of detection and localization of damage. The next step following the damage detection is the assessment of the damage repercussion on the performance and operational life of components or systems. This extension of NDE, which includes the steps of diagnosis and prognosis, is often known as structural health monitoring (SHM) [1]. The guided wave (GW) technique is one of the most well-known SHM methodologies to interrogate components and structures. The technique is based on the analysis of stress waves propagating through the component to identify damage. Almost all SHM systems based on GWs use active transducers to excite specific stress wave modes and interrogate the component.

Piezoelectric wafer active sensors (PWAS) are inexpensive transducers that operate on the piezoelectric principle. PWAS has been developed to generate and detect elastic waves in metallic and composite materials. PWAS are attached to the host structure through an adhesive bonding layer and generate and detect Lamb waves in the structure by means of in-plane strain coupling [2]. An alternative to PWAS for the generation of GWs is piezoelectric polymers [3, 4]. Piezoelectric-polymer composites were first developed as transducers to achieve mechanical and electrical properties, which cannot often be obtained with single phase materials [5]. In recent years, an important number of thin piezoelectric-polymer composites have been developed in order to obtain flexible materials to be used as transducers [6, 7, 8, 9]. The electrical, magnetic and mechanical properties of polymer composite materials can be tuned adjusting the filler concentration. Features of these materials include their ease of production, which makes it possible to obtain different sizes and shapes [7], capability of covering large areas, applicability to any surface shape (planar, curved or even with irregularities), absence of bonding layer between sensor and substrate, usage as self-powered sensor and adjustability of the composite properties [5]. During the manufacturing of such composites, the most important requirement is to obtain a flexible and soft material in the adequate thickness range, while maintaining good piezoelectric properties [6].

In this paper, the development of a sensor placement technique based on the image differential method is presented. For that, a FEM model has been constructed using the software Comsol. The model consists of a thin aluminum test coupon with three holes where a crack of tolerable length has originated from one of the holes due to fatigue loading. A network of coated piezoelectric composite transducers is generated to monitor the crack growth. The transducer pattern is defined from the output of guided wave FEM simulations. A damage index is defined in order to quantify the signal difference between the structure in the pristine and damage condition. A correlation between the damage index and the damage level is found.

1.1 FEM Modeling and Simulation of Guided Waves

The numerical simulation is a powerful tool to understand the phenomena of propagation and interaction of GWs with features and defects in a material [10]. The finite element method (FEM) can be used to model ultrasonic wave propagation in materials. The use of numerical simulation enables the modification of important parameters which otherwise could not be changed, such as the electromechanical and physical properties of materials, it

also makes it possible to easily modify the geometry of the structure analyzed [11].

2D FEM models were developed to study the generation of guided waves in an aluminum plate [12]. It was found that simulation of the electromechanical coupling between a PZT wafer transducer and the structure offers more accurate results than the use of a point source for the generation of GWs. In fact, when forces or moments are applied to generate guided waves the real complex situation of wave composition and interaction is simplified [13].

1.2 Damage Detection

An interesting approach for damage detection is the signal differential method [14]. This method consists in recording the signals of the undamaged condition, which are obtained for a specific combination of actuators and sensors, and then subtracting those signals from the signals taken for the structure while in operation. Both the amplitude and phase information of the signal should be taken into account. This method is particularly suitable for damage detection when echoes from the crack are mixed with backscatter from the boundaries. The effect of the presence of cracks is visible in the resulting signal. The method also allows the location of spots where the differential signal is sensitive to the presence of damage for a specific combination of actuators and sensors. This information could also be applied for the placement of sensors, in which case the signal differential method becomes the basis for damage monitoring.

An extension of the signal differential method is the image differential method [15] in which the wave propagation at each time step is recorded for the undamaged condition and is subtracted from the signals of the damaged condition, with the result being presented in either 2D or 3D images. The wave propagation could be represented by the x, y or z displacement. This method not only can be used for damage detection but also gives information about the location of maximum differential displacement spots.

1.3 Sensor Placement

In SHM systems based on GWs the number of transducers and their placement on the structure are important parameters to be defined [16]. In general it can be stated that the more transducers are placed on a structure, the more accurate is the data that can be generated about the structure's health condition. In real applications, the number of available sensors is limited due to the mass of data to be handled, the monitoring system's mass and complexity, budget constraints, among others. Taking the limited number of transducers available into account, their placement should be optimized in order to record as much data of the structural health condition as possible [17]. The optimum sensor placement (OSP) is typically approached as a constrained optimization problem in which the criterion to be maximized is the probability of a specific sensor to detect damage in a specific location. The solution should be a sensor layout, given a certain quantity of sensors as input, that provides as much information on the structural health condition as possible. Moreover, most of damage detection algorithms are able to locate damage only after it has been detected. It is often difficult and time consuming to solve OSP problems due to the complexity of the function to be optimized and the large number of variables involved [16]. The proposed image differential method not only can be used for damaged detection, but also gives information about the location of maximal differential displacement spots, which can be used for the placement of sensors.

2 SIMULATION PROCEDURE

The material studied as an FEM simulation case was aluminum (E = 69 GPa, ρ = 2.7 g/cm^3, ν = 0.33, mass damping coefficient = 0, stiffness damping coefficient = 0). A boundary pressure load was applied to a disc with diameter of 7 mm on the upper surface of the plate for the generation of both symmetrical (S_0) and anti-symmetrical (A_0) Lamb wave modes. All the boundaries of the model were set to be free. The excitation signal was a Hanning-windowed five-cycle sinusoidal function with a central frequency set at 440 kHz. The mesh of the model was generated automatically by the software with free tetrahedral elements, which were chosen to be uniform throughout the model. Simulations were performed in the time dependent mode with a time space of 1x10^{-7} s, the average element quality was set to 0.66. In a first version of the simulation, model M1, a time of flight (TOF) analysis was made. The results obtained were compared to those obtained in a practical experiment. In model M2 a sensor placement strategy based on the image differential method is discussed with respect to successfully monitoring crack growth.

2.1 Model M1. TOF Analysis

Basic principles of acoustic wave propagation were verified in the model M1. This model takes into account the electromechanical coupling between a PZT wafer transducer and the structure. A 500x250x1.5 mm aluminum plate was analyzed. PWAS were modeled with coupled field elements in the shape of discs with 7 mm in diameter and 200 µm in thickness. Five PZT transducers (S1 – S5) were placed on the top surface of the plate, each at an increasing distance of 50 mm from the point source, as shown in Fig. 1(a). The time difference between the excited signal and the arrival of the wave-package to the sensor represents the time of flight (TOF). The simulated voltage signals were recorded at each sensor. Practical experiments were conducted to validate the simulation results. An aluminum plate was instrumented with five PWAS (American Piezo Ceramics, APC-850) with 7 mm in diameter and 200 µm in thickness. The PWAS where applied to the plate following the recommended surface preparation [18] and using the M-Bond 610 adhesive. The dimensions of the plate and the positions of the five PWAS sensors were in agreement with the model M1. The function generator of a VirtualBench (National Instruments, VB-8012) was used to generate a Hanning-windowed five-cycle sinusoidal function with a central frequency set at 440 kHz. The signal was sent through a power amplifier to the actuator PWAS (Fig. 1(b)). The response signals from the sensor PWAS were recorded by the signal oscilloscope of the VirtualBench. An algorithm was elaborated with the Labview software to simultaneously generate the excitation signal and record the response signal from the sensors.

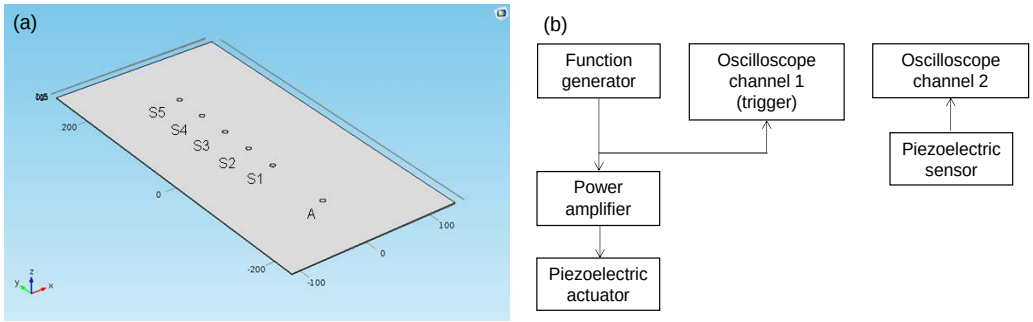

Figure 1. (a) Model M1 indicating the position of the actuator (A) and sensors (S1 – S5). (b) Schematic representation of the experimental setup.

2.2 Model M2. Image Differential Method and Sensor Placement

In model M2 an aluminium plate of 400x112x1.5 mm containing three holes with a diameter of 7.5 mm were made to simulate rivet holes (Fig. 2(a), (b)). In order to simulate damage, a crack of 10.25 mm in length and 1 mm in thickness was generated (Fig. 2(c)). Displacements resulting from the guided waves at the top surface of the plate were determined for both damaged and pristine conditions. Afterwards, an algorithm based on the signal differential method was applied in order to isolate the signal originated by the wave reflections at the crack, which constitutes the differential image. The differential images were presented in a 2D colored map, which has been used to define the position and shape of receiving sensors used in a pitch-catch configuration to detect the damage.

As input for the physical and electromechanical properties of the sensors the properties of the $BaTiO_3$/epoxy composite were used [19]. The mechanical properties of the sensors were assumed to be isotropic. The thickness of the sensors was set to be 200 µm. The bottom surface of the sensors was grounded. Boundary probes were applied to obtain the response signals, where the voltage was measured at the top surface of the sensors.

In order to automatically quantify the health of the structure based on the information provided by the sensors, a damage index (DI) was defined. The root mean square deviation (RMSD) was the DI chosen for this purpose. The statistical comparison between the signals of the structure in the pristine and damaged condition results in the RMSD DI, which is a scalar quantity. The presence of damage produces a difference between the signals of the damaged and pristine conditions, which is then quantified by the RMSD DI [20]. This technique is ideal for damage detection since the information recorded by the signals carries both the amplitude and the phase changes arising from the damage. The RMSD DI is defined as the relative ratio of the difference between each measurement and baseline signals as follows [21]:

$$RMSD = \sqrt{\frac{\sum_N (s_i - s_i^0)^2}{\sum_N (s_i^0)^2}}$$

where i s is the ith measurement, 0 indicates the baseline signal and N is the data length. In this paper the effect of damage growth on the RMSD DI was studied. For that, increasing damage stages (crack lengths of L1 = 4.1 mm, L2 = 8.2 mm, L3 = 12.3 mm, L4 = 16.4 mm) were simulated in the M2 model. Then the RMSD DI of the structure was calculated for each crack length and a correlation between the RMSD DI and crack length was found.

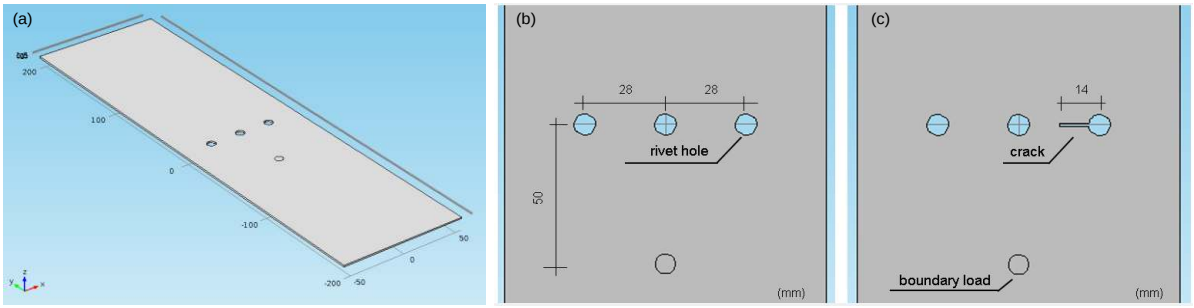

Figure 2. Model M2 in (a), (b) the pristine condition and (c) damaged condition.

3 RESULTS AND DISCUSSION

3.1 Model M1. TOF Analysis

The simulated signals recorded by the sensors placed on the plate surface according to Fig. 1(a) are shown in Fig. 3(a). Each row displays a wave package sent by the boundary source followed by wave packages resulting from the boundary reflections at the plate edges. A straight-line correlation (R^2 = 100 %) was obtained between the distance covered and the TOF of the first wave package. The slope of this line is the group velocity of the S_0 mode, running at a speed of 5319 m/s. Fig. 3(b) shows the experimental results. Each row displays first the electromagnetically coupled excitation, then the direct wave package sent by the actuator PWAS, followed by wave packages resulting from boundary reflections at the plate edges. The group velocity obtained in the simulation is in good agreement (relative error = 0.78 %) with the experimental results, which showed a S_0 group velocity of 5361 m/s. A straight-line correlation (R^2 = 99.99 %) was also obtained between the distance covered and the TOF. Due to the slightly higher value of S_0 group velocity obtained in the experimental results, there is a difference in the arrival time of the wave packages when compared to the simulated and experimental response of the sensor S1, as shown in Fig. 3(c). The wave packages followed different paths due to boundary reflections before arriving to the sensors (Fig. 3(d)).

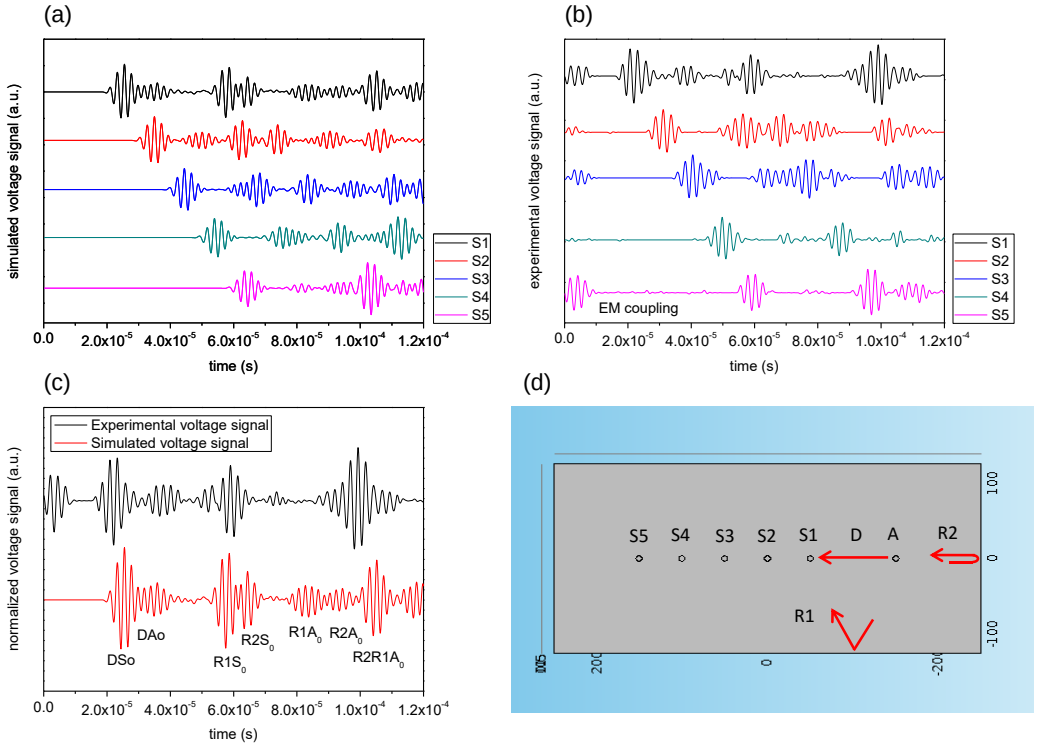

Figure 3. (a) Voltage signals recorded by the sensors of the M1 model obtained through simulation. (b) Voltage signals recorded during the experimental tests. (c) Comparison of the signals recorded by the sensor S1 in the simulation and experimental tests. (d) Schematic of the wave paths for each wave package, (D) direct wave, (R1, R2), boundary reflections.

These experiments were repeated at frequencies of 100 kHz and 234 kHz, for which high amplitude ratios occur according to the dispersion diagram, for the A_0 mode at 100 kHz and 440 kHz, and for the S_0 mode at 234 kHz respectively. A very good correlation between the simulation and experimental results was obtained for the group velocities of the two modes. In all cases, the group velocities of the FEM model differed slightly from the experimental results. The simulated A_0 group velocity runs slightly faster and the S_0 group velocity slightly slower than the respective velocity obtained from the experimental results. It is known that when forces are applied to generate guided waves, being the case in the model, the real complex situation of wave composition and interaction is simplified [13]. The modelling of transducers with coupled elements produces more accurate results than using a force point for the generation of GWs. In order to solve this problem, efforts are being made to develop a fully coupled model, in which actuators and sensors are modelled by piezoelectric elements.

3.2 Model M2. Image Differential Method and Sensor Placement

The propagation of the simulated guided waves is shown in Fig. 4. These snapshots of the top view of the model were taken at $20x10^{-6}$ s. The actuator modeled by a boundary pressure load is able to produce an omnidirectional wave front. The interaction of the wave front with discontinuities of the plate (rivet holes, defect and plate edges) creates a complex displacement pattern due to reflection, transmission and as a result the formation of constructive and destructive interferences. To generate the differential images, GW displacement patterns of the out-of-plane displacement were recorded in both the pristine and damaged conditions and the difference between them was obtained at each time step having been recorded for up to $100x10^{-6}$ s.

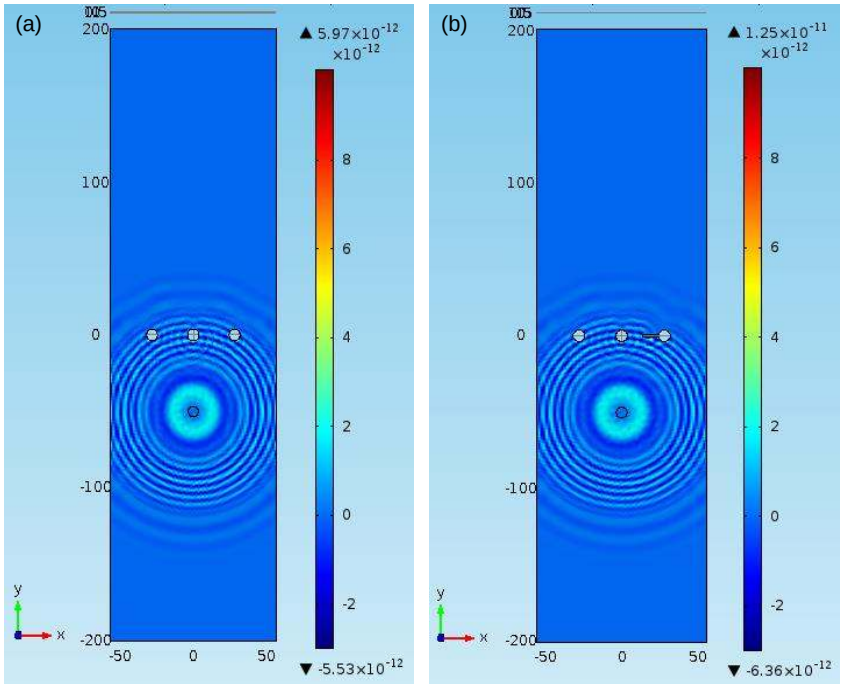

Figure 4. Top view of the model M2 showing out-of-plane displacement patterns. Snapshots taken at $2.0x10^{-6}$ s for the (a) pristine condition and (b) damaged condition.

The differential images, presented in Fig 5, show the propagation of the isolated waves reflected at the crack tip. The behavior of the spots of high differential displacement as a function of time was studied with differential images for up to $100x10^{-6}$ s having been analyzed. In Fig. 5(b) it is possible to observe that the maximum in differential displacement occurs at $27x10^{-6}$ s.

The influence of the crack length on the behavior of the spots of high differential displacement was also analyzed. For that, differential images were constructed according to the model M2 (Fig. 2(c)) with increasing levels of damage (crack lengths of L1 = 4.1 mm, L2 = 8.2 mm, L3 = 12.3 mm, L4 = 16.4 mm). The behavior of the spots of high differential displacement as a function of the crack length is shown in Fig. 6. The reflection at the crack tip of the waveforms from the actuator increases with the crack length, resulting in an increment of the area of spots of high differential displacement. The spots are concentrated on the top and bottom regions of the crack. Placing passive sensors at spots of high differential displacement is of interest to obtain high amplitude signals in order to detect damage growth in a reliable manner in accordance to the conditions of the model.

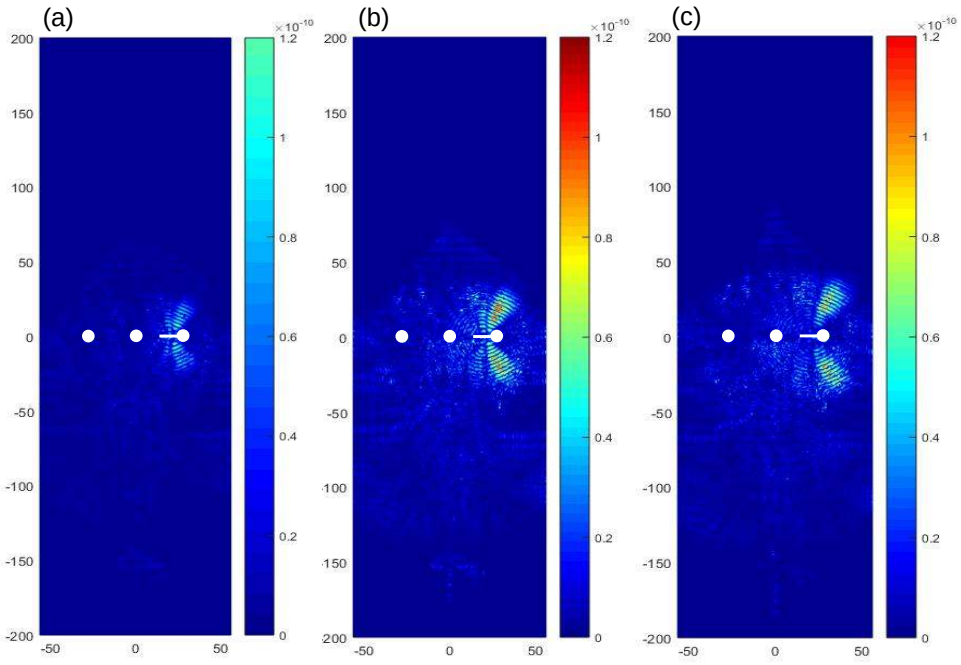

Figure 5. Differential images of the M2 model taken at (a) $25x10^{-6}$ s (b) $27x10^{-6}$ s, (c) $29x10^{-6}$ s. The warm colors (red to yellow) indicate spots of high differential displacement.

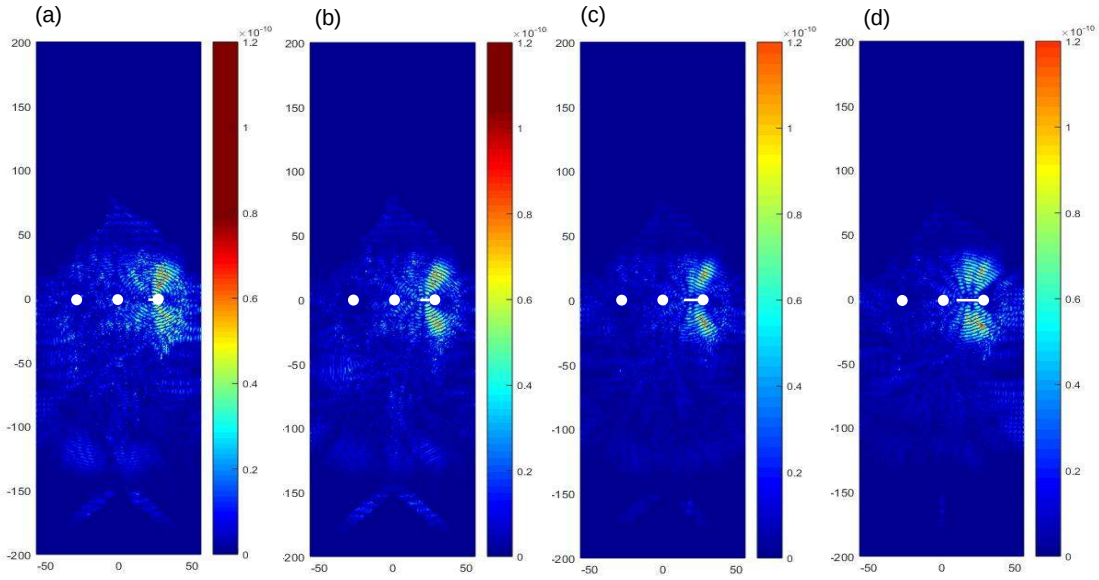

Figure 6. Influence of the crack length on the spots of high differential displacement for the M2 model with crack lengths of (a) L1= 4.1 mm, (b) L2 = 8.1 mm (c) L3 = 12.3 mm (d) L4 = 16.4 mm. Images taken at $27x10e^{-6}$ s.

By applying image processing techniques, the contours of these spots were extracted from the differential images and exported to the Comsol software for the construction of a pattern of sensors according to these shapes, where the results are shown in Fig. 6. The novelty of this approach regarding sensor placement is that the physical phenomena of wave propagation and interaction with discontinuities of the analyzed structure are taken into account for the selection of the geometry and placement of the sensors. Still, parameters such as sensor surface area and sensor thickness as a function of the excitation frequency need to be optimized in order to ensure optimal energy transduction and coupling with the ultrasonic-guided waves traveling in the structure [22].

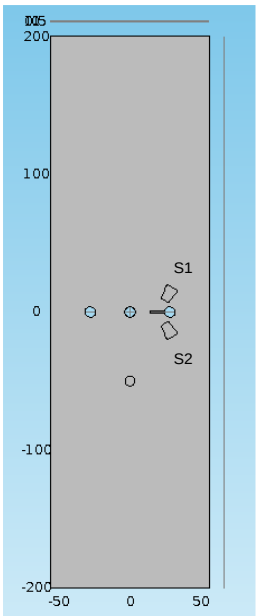

Figure 7. Sensor pattern constructed based on the image differential method to detect damage growth for the conditions of the model M2.

The simulated voltage signals of the S1 sensor as a function of the crack length are shown in Fig. 7(a). The crack length L0 corresponds to the pristine condition. Based on these results, the differential voltage signals were obtained, which are shown in Fig. 7(b). The RMSD DI was calculated for the sensors (S1, S2) of the sensor pattern at each crack length (L1 – L4), where the results are shown in Fig 8(c) and (d). The RMSD DI changes significantly with the damage growth. The DI increases monotonically as the damage stage increases for the range of crack length studied. A straight line correlation (R^2 = 99.97 % for S1, R^2 = 98.14 % for S2) was obtained in both cases. These calibration curves could allow the estimation of the damage stage of the structure, defined in terms of the crack length. For that, the voltage signals of the sensor pattern for the structure in the service conditions are required. Efforts are being made to obtain experimental signals from the sensor pattern developed made of $BaTiO_3$/epoxy resin composite in order to validate the calibration curve and calculate the precision of this method to estimate the damage state of the structure.

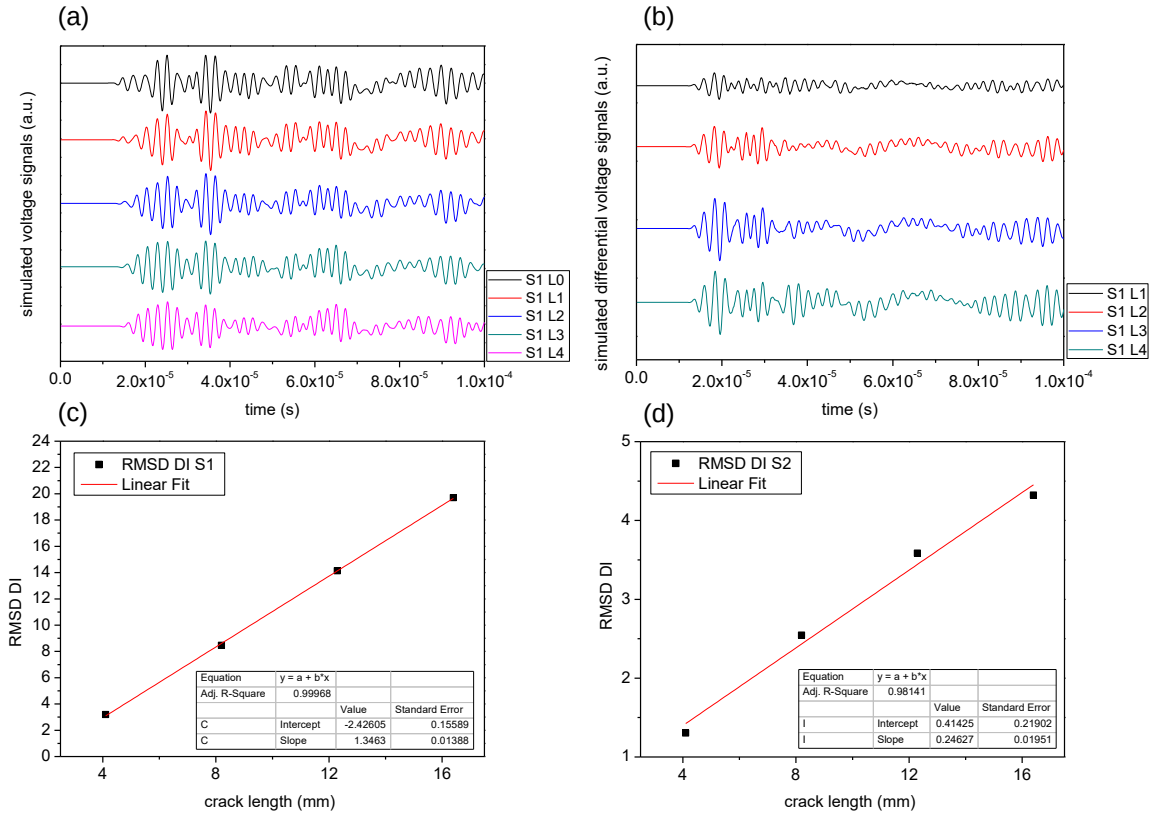

Figure 8. (a) Simulated voltage signals acquired by the S1 as function of the crack length (L1-L5, L0 = pristine condition). (b) Simulated differential voltage signals obtained by the signal differential method. Calibration curve constructed for damage detection for the sensor (c) S1 and (d) S2 according to Fig. 7.

4 CONCLUSIONS

In this paper the results of the development of a FEM model based on the propagation of GWs to study SHM techniques using PWAS and BaTiO3/epoxy resin piezoelectric composites are presented. The 3D FEM simulation model built using the Comsol software allowed the analysis of the propagation and interaction of GWs with features and defect of an aluminium plate. TOF analysis was executed at several frequencies to obtain the group

velocities of the generated S_0 and A_0 Lamb wave modes. A good agreement was obtained between the simulation and experimental results although small discrepancies were found in the value of the group velocities. In order to further develop the FEM model, the construction of a fully coupled model, in which actuators and sensors are modelled by piezoelectric elements, is taking place. The image differential method, which is based on the signal differential method, was introduced for the generation of 2D image sequences determined from FEM, where images resulted from the difference in the wave propagation pattern between the undamaged and damaged conditions of the analyzed structure. This method allowed the localization of spots of high differential displacement, which was then used to construct a sensor pattern to detect damage growth in a reliable manner for the conditions of the model. As input data for the physical and electromechanical properties of the sensor pattern, previous results of the characterization of the $BaTiO_3$/epoxy resin piezoelectric composite were applied. The signal difference between the structure in the damaged and pristine conditions was quantified using the RMSD damage index. A straight line correlation was found between the RMSD DI and the crack length. These calibration curves could allow the estimation of the damage stage of the structure having as an input the voltage signals generated by the sensor pattern.

Important features of the sensor pattern, such as sensor surface area and sensor thickness, need to be optimized in terms of the excitation frequency to ensure optimum energy transduction and coupling with the ultrasonic-guided waves traveling in the structure. The validation of the simulation results needs to be carried out by means of comparison with experimental results. Furthermore, the operational and environmental variations of the monitored structure need to be addressed since signals change due to varying operational and environmental conditions of the structure such as temperature, humidity, and others possibly.

REFERENCES

[1] V.M., Karbhari, Non-Destructive Evaluation (NDE) of Polymer Matrix Composites - Techniques and Applications. Chapter 1 *"*Introduction: the future of non-destructive evaluation (NDE) and structural health monitoring (SHM)*"*. Ed. Elsevier (2013).

[2] L. Yu, G. Bottai-Santoni, V. Giurgiutiu, Shear lag solution for tuning ultrasonic piezoelectric wafer active sensors with applications to Lamb wave array imaging. International Journal of Engineering Science, **48**, 848–861, 2010.

[3] V.T. Rathod, et al., Characterization of large-area PVDF thin film for electro-mechanical und ultrasonic sensing applications. Sensors and Actuators A, **163**, 164–171, 2010.

[4] J.M. Park, et al., Nondestructive damage detection and interfacial evaluation of single-fibers/epoxy composites using PZT, PVDF and P(VDF-TrFE) copolymer sensors. Composites Science and Technology, **65**, 241–256, 2005.

[5] I. Payo, and J.M. Hale, Sensitivity analysis of piezoelectric paint sensors made up of PZT ceramic powder and water-based acrylic polymer. Sensors and Actuators A, **168**, 77–89, 2011.

[6] Z.M., Dang et al., Flexible nanodielectric materials with high permittivity for power energy storage. Advanced Materials, **25**, 6334–6365, 2013.

[7] I. Babu and G. de With, High flexible piezoelectric 0-3 PZT-PDMS composites with high filler content. Composites Science and Technology, **91**, 91–97, 2014.

[8] M. Dietze and M. Es-Souni, Structural and functional properties of screen-painted PZT-PVDF-TrFE composites. Sensors and Actuators A, **143**, 329–334, 2008.

[9] D. Carponcin et al., Integrated function in a high thermostable thermoplastic PZT/PEEK

composite. Journal of non-crystalline Solids, **388**, 32–36, 2014.
[10] B. Ghose and K. Balasubramaniam, Finite element modelling and simulation of ultrasonic guided wave propagation using frequency response analysis. Proceedings of the 14th Asia-Pacific Conference on NDT, 2013.
[11] J. Soderkvist, Using FEA to treat piezoelectric low-frequency resonators. IEEE transactions on ultrasonics, ferroelectrics, and frequency control, **45**, 3, 1998.
[12] J.H. Nieuwenhuis et al., Generation and detection of guided waves using PZT wafer transducers. IEEE Trans. Ultrason. Ferroelectr. Freq. Control, **52**, 2103–11, 2005.
[13]W. Liu and V. Giurgiutiu, Finite Element Simulation of Piezoelectric Wafer Active Sensors for Structural Health Monitoring with Coupled-Filed Elements Sensors and Smart Structures Technologies for Civil, Mechanical, and Aerospace Systems. Proc. of SPIE, **6529**, 2007.
[14] V. Giurgiutiu, Structural Health Monitoring With Piezoelectric Wafer Active Sensor. Chapter 10 *"Wave Propagation SHM with PWAS"*. Elsevier Academic Press, (2008).
[15] R. Sridaran Venkat, C. Boller, N.B. Ravi, C. Nibir, D.R Mahapatra, Simulation von Sensorsystemen zur Inspektion von Bauteilstrukturen im Sinne eines Structural Health Monitoring. Proc. Annual conference of German Society for Non-destructive testing (DGZFP), 2015.
[16] C. Fendzi, et al., Optimal sensors placement to enhance damage detection in composite plates. Proc. 7th European Workshop on Structural Health Monitoring, **24**, 1981–1988, 2014.
[17] H. Sun and O. Büyüköztürk, Optimal sensor placement in structural health monitoring using discrete optimization. Smart Mater. Struct, **24**, 125034, 2015.
[18] Vishay micro-measurements. Instruction Bulletin B-129-8. Surface Preparation for Strain Gage Bonding http://ww2.bse.vt.edu/kumar/Instrumentation/Straingauge/Strain%20Gauge%20Surface%20Preparation.pdf
[19] O. Bareiro, R. Sridaran Venkat, J. Adam, C. Boller, Development of the fabrication process and characterization of piezoelectric $BaTiO_3$/epoxy composite to the used for coated ultrasonic transducer patterns in structural health monitoring. Proc. 19th World Conference on Non-Destructive Testing. 2016
[20] V. Giurgiutiu, Structural Health Monitoring with Piezoelectric Wafer Active Sensors, 2nd Edition. Chapter 10 *"High*-Frequency Vibration SHM with PWAS Modal Sensors – *the Electromechanical Impedance Method".* Elsevier Academic Press (2014).
[21] M. Gresil, V. Giurgiutiu, Y. Shen, Predictive Simulation of Structural Sensing. Collection of Technical Papers - AIAA/ASME/ASCE/AHS/ASC Structures, Structural Dynamics and Materials Conference, 2012.
[22] B. Lin and V. Giurgiutiu, Power and energy transduction analysis of piezoelectric wafer-active sensors for structural health monitoring. Structural Health Monitoring, **11**, 109–121, 2011.